Physica Medica 60 (2019) 22–29

Contents lists available at ScienceDirect

Physica Medica

journal homepage: www.elsevier.com/locate/ejmp

Original paper

Enhancement of linear energy transfer in gold nanoparticles mediated radiation therapy

Sherif M. Gadoue[a,*], Dolla Toomeh[b]

[a] Department of Physics and Applied Physics, University of Massachusetts Lowell, Lowell, MA 01854, USA
[b] Department of Radiation Oncology, University of Washington School of Medicine, WA 98195, USA

ARTICLE INFO

Keywords:
Nanoparticles
LET enhancement
Dose enhancement

ABSTRACT

Objective: The metric dose enhancement ratio (DER) has been widely used to assess the enhancing capability of gold nanoparticles (GNPs). However, there is a large disparity between the observed radiobiological outcome and DER values. A new metric, linear energy transfer enhancement ratio (LETER), is introduced to bridge the gap between theoretical predictions and the experimentally measured sensitization.
Methods: The radiation transport code SCEPTRE is used to examine the efficacy of the proposed new metric. Different clusters of GNPs irradiated with x-ray photons generated at 120 kVp and therapeutic 6 MV photon beams are investigated. For each pattern, two GNPs sizes are examined 50 and 100 nm.
Results: An enhancement in the linear energy transfer has been observed for both energies. In the case of 120 kVp, LETER is substantially lower than DER; moreover, it decreases with increasing GNP size. On the other hand, the results of 6 MV show that LETER is relatively higher than DER, and it increases with the size of GNP. For the studied energies, LETER is in good agreement with the sensitization reported in the literature.
Conclusion: The results indicate the merit of LETER as a better indicator of the radiobiological outcome of GNP aided radiotherapy.

1. Introduction

In the last decade, there has been a growing interest in using nanoparticles as radio-sensitizers in radiotherapy for cancer treatment [1]. The ultimate goal of radiation therapy, in practice, is to maximize the dose to cancer cells while, simultaneously, sparing the surrounding healthy tissues [2]. This can be achieved using different techniques, one such method, that has received increasing attention in recent years, is gold nanoparticles (GNPs) aided radiation therapy [3].

The underlying mechanism behind GNP sensitization is predicated on radiation dose escalation in the local nanoscale neighborhood of irradiated GNPs due to the increased production of secondary electrons [4]. For incident photon energy below 500 keV, the photoelectric effect is the dominant photon interaction in gold [2,5]. Following photoelectron emission, a single or a cascade of Auger electrons is released from GNP [4–6]. Low energy photo- and Auger electrons, with sufficient energy to leak out from the GNP surface, will deposit the majority of their energy locally in the nanometric vicinity of GNP [1]. In this perspective, compared to the case where GNP is not present, there is a boost in radiation dose and the extent of such increase is invariably quantified via the metric dose enhancement ratio (DER) defined as

$$\mathrm{DER} = \frac{\text{dose delivered to the medium with GNP}}{\text{dose delivered to the medium without GNP}} \quad (1)$$

Thus far, DER is the golden yardstick employed in the literature to exclusively assess the efficacy of GNPs. Several studies have been carried out to determine the DER for numerous sizes of GNP and different incident photon energies using various Monte Carlo radiation transport codes, [2,7–10] and deterministic methods [5,11]. Yet, the observed sensitization of GNPs in vitro does not agree quite well with the theoretical computations of DER [12,13]. For example, the observed biological effect in MV beams is higher than the theoretical calculations; furthermore, for kV photons, the experimentally reported sensitization is much less.

The local effect model (LEM) has been used by some researchers to resolve the aforementioned discrepancy. For example, McMahon et al. compared the experimental cell survival of MDA-231 cells exposed to 160 kVp, 6 MV and 15 MV photons with LEM predictions and reported that such predictions are in good agreement with experimental results [6,14]. Although this approach is successful in some situations, it lacks some key features which are pivotal for a thorough evaluation of GNPs efficacy. For instance, the radiation dose input to the model has been calculated using Monte Carlo computations in concentric spherical

* Corresponding author.
E-mail address: smgadoue@gmail.com (S.M. Gadoue).

https://doi.org/10.1016/j.ejmp.2019.02.019
Received 21 November 2018; Received in revised form 16 January 2019; Accepted 23 February 2019
Available online 22 March 2019

shells, thus neglecting the anisotropy effects observed in GNP-mediated radiation therapy [5]. Moreover, the distribution of GNPs in the simulation has been assumed to be uniform which is justifiably arguable since GNPs tend to cluster and agglomerate at the cellular level [11,15].

In order to bridge this disconnect and gain a better understanding of the radio-sensitizing effects of GNPs, an additional metric is needed to relate the physical dose deposited in cells to the radiobiological outcome. Of special interest in connection with the biological effects of radiation is the linear energy transfer (LET), which is defined as the average energy lost per unit track length of charged particles. According to the definition, it can be realized that electrons with higher LET values will exhibit denser ionizing events along their track which is reflected into more significant biological consequences.

Several studies have used Monte Carlo simulations to calculate the average LET of proton beams [16,17] and secondary electrons produced by x-rays [18]. Furthermore, it has been shown that there is a substantial increase in the LET of secondary electrons in the vicinity of a GNP exposed to kVp beams [18], and that, in particular, LET may be enhanced at high-Z/soft tissue interfaces [19,20].

However, computing the average LET in the nanoscale remains a big challenge in Monte Carlo simulations for several reasons. In order to capture the angular anisotropy [5], as well as the large gradients of the dosimetric quantities of interest in the immediate vicinity of GNP, an unrealistically large number of nanoscopic tally volumes in the form of burdensome spherical sections should be used. In view of the infinitesimally small scoring volumes, this will result in impractically long running times and the subsequent computations will suffer from high statistical uncertainties.

Alternatively, deterministic methods represent a more efficient approach in the field of nanoscale simulations and have been proven to be very favorable for this class of problems as demonstrated by Gadoue et al. [5,11,21]. For example, a deterministic radiation transport code has been used to obtain detailed 3D DER distribution around GNPs, the resulting high-resolution profiles have shown that DER is anisotropic; a feature that cannot be resolved otherwise.

Despite its importance in quantifying GNP efficacy, LET enhancement ratio (LETER) has not been addressed in the literature so far. This work is carried out, for the first time, to compute LETER profiles in the immediate vicinity of GNPs using the radiation transport code SCEPTRE. The experimentally observed sensitization is compared with the obtained LETER values to show its applicability in predicting the biological impact of GNPs. The results of the simulations demonstrate not only the prognostic nature of LETER, but also its ability to coherently answer the controversial questions.

2. Methods

2.1. Geometry

As shown in Fig. 1, the geometry used in this study consists of an outer sphere of normal tissue having a radius of 5.5 cm. An inner sphere of radius 1.5 cm, representing the tumor, lies within the outer sphere. Incident photons are impinging on the outer sphere from the left in a plane-parallel direction with a diameter of 3 cm. X-ray photons generated at 120 kVp from a tungsten target with an aluminum filtration of 3 mm (representative of diagnostic beams), and 6 MV photons (representative of therapeutic beams) are investigated. A pre-measured spectrum of both energies has been used in the simulation. Two GNP sizes are considered, 50 and 100 nm diameter, and the composition of GNP is assumed to be 100% gold.

2.2. Simulations

In the last few years, many software packages that solve the Boltzmann transport equation deterministically have been released. More recently, Sandia National Laboratories released a next-generation code, Sandia Computational Engine for Particle Transport for Radiation Effects (SCEPTRE), which is a general purpose deterministic code that has unique features. SCEPTRE version 1.7 represents a significant advance in the field of deterministic computations [22]. The solution method is based on unstructured finite element methods to resolve the spatial dependence, while the energy discretization is achieved by the multi-group formalism. The available angular treatment methods are the discrete ordinates and spherical harmonics. For more computational efficiency and greater accuracy, SCEPTRE allows the user to construct the optimal solution method for each energy group. The number of energy groups used is 50, the group structure is linear for photons and logarithmic for electrons. The calculation utilized the discrete ordinates S_{16}, and a convergence tolerance of 10^{-8}. The cross section libraries used in the transport calculations are generated using CEPXS, available in the integrated tiger series (ITS) code package [23]. The lower energy cutoff for both photons and electrons is set to 1 keV. The calculation of LET is carried out by averaging the LET of secondary electrons over the fluence distribution or the dose distribution [17,24,25]. Fluence-averaged (sometimes called track-averaged) and dose averaged LET are computed according to the following:

$$LET_{fluence}(\vec{r}) = \frac{\int\int \phi(\vec{r}, E) LET(\vec{r}, E) \mathrm{d}E\mathrm{d}V}{\int\int \phi(\vec{r}, E) \mathrm{d}E\mathrm{d}V} \quad (2)$$

$$LET_{dose}(\vec{r}) = \frac{\int\int D(\vec{r}, E) LET(\vec{r}, E) \mathrm{d}E\mathrm{d}V}{\int\int D(\vec{r}, E) \mathrm{d}E\mathrm{d}V} \quad (3)$$

where $\phi(\vec{r}, E)$ is the secondary electron scalar flux at position $\vec{r}$, and

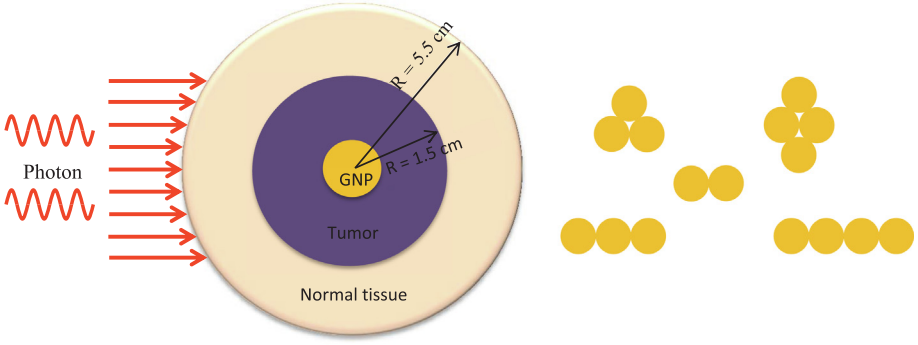

Fig. 1. (a) Schematic geometry of the problem. (b) Cluster patterns studied, dimensions are not to scale.

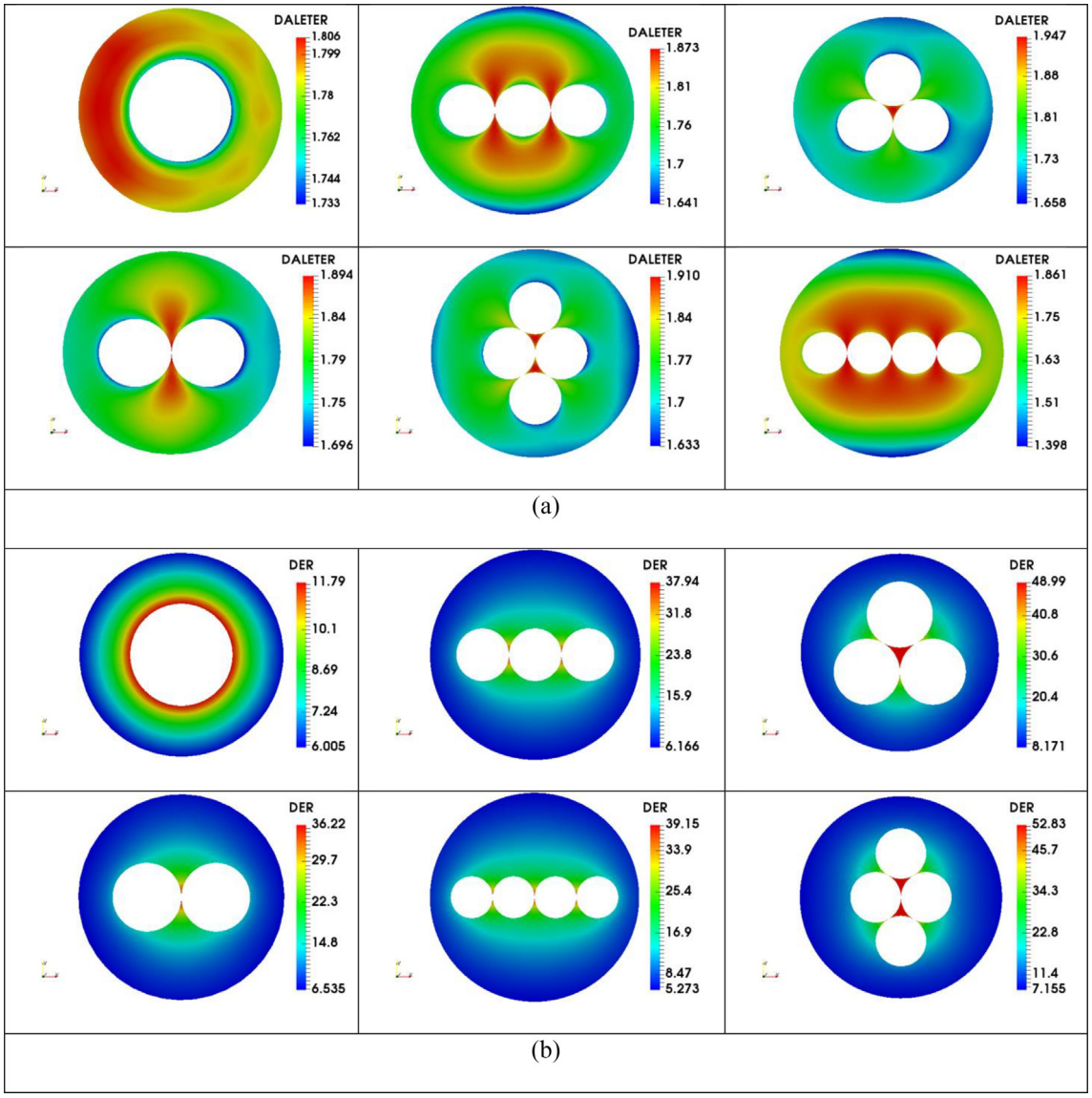

Fig. 2. Different metrics due to electrons in a 25 nm annular region around 50 nm GNP when exposed to x-ray photons generated at 120 kVp. (a) DALETER (b) DER.

$D(\vec{r}, E)$ is the dose distribution due to secondary electrons at position $\vec{r}$. The integration is carried out over the voxel volume and for all electron energies.

The proposed metric, LET enhancement ratio (LETER) can be defined as

$$\text{LETER} = \frac{\text{Average LET due to secondary particles in the presence of GNP}}{\text{Average LET due to secondary particles without GNP}} \quad (4)$$

where the average is based on either the fluence or the dose distribution. The enhancement in LET will be denoted FALETER if the average is fuence-based, and DALETER if it is dose-averaged. Owing to its more relevance to biological effects, DALETER will be investigated in this study instead of FALETER.

3. Results

Fig. 2 shows the DALETER and DER in an annular region of thickness 25 nm, due to secondary electrons emerging from 50 nm GNPs when irradiated with x-ray photons generated at 120 kVp. As can be seen from the figure, the values of DER are very high ranging from 5.273 to 52.83, whereas the values of DALETER are much smaller in the range of 1.398–1.947. Furthermore, there is an obvious anisotropy in the case of a single GNP, where the LET enhancement in the reverse direction (proximal) is slightly higher than it is for the forward direction. However, this angular asymmetry is alleviated, to a certain degree, as GNPs aggregate in clusters.

Interestingly, some patterns exhibit relatively higher LET enhancement values compared to the other clusters. For instance, a linear chain of two GNPs provides more LET enhancement rather than a three-GNPs chain. In addition, a closely packed triangular pattern is more effective than a four-GNP rhomboid cluster. This is mainly attributed to the fraction of low-energy electrons in the secondary-electron spectrum; in fact, these specific patterns have a greater contribution from the lower energy electrons as opposed to the other clustering patterns. Since low-energy electrons have higher values of LET, these patterns will evidently possess higher LET enhancement values.

As can be anticipated, more closely packed patterns provide more LET enhancement compared to their linear counterpart in a similar fashion to the DER profiles. For instance, the triangular shape has an LET enhancement that ranges from 1.658 to 1.947, whilst a three linear chain provides a range of 1.641–1.873 only. Moreover, there exist obvious hot spots in the profiles of these special patterns developed locally in the region between mutually contiguous GNPs due to the additive

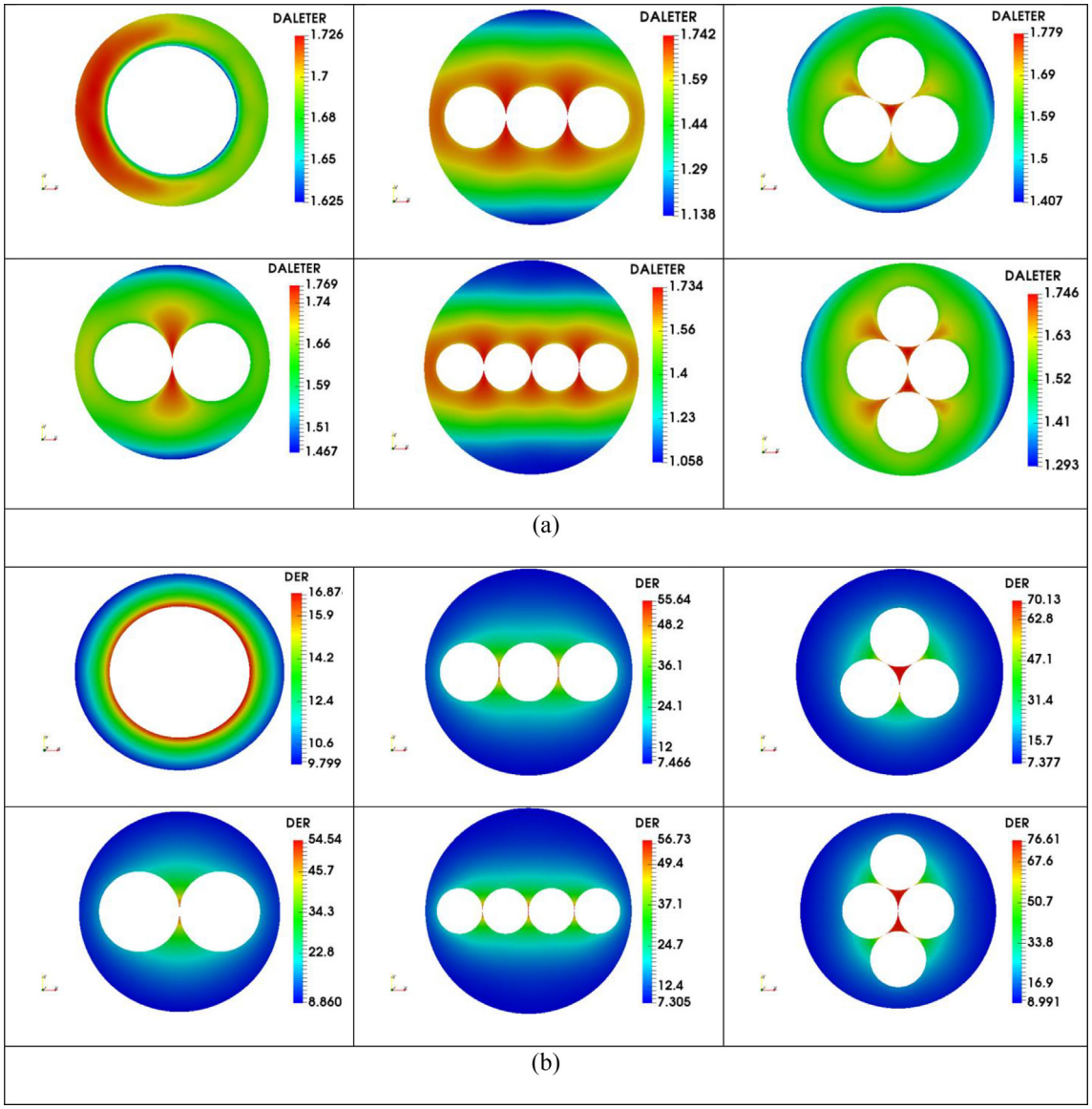

Fig. 3. Different metrics due to electrons in a 25 nm annular region around 100 nm GNP when exposed to x-ray photons generated at 120 kVp. (a) DALETER (b) DER.

effects of secondary electrons.

Fig. 3 illustrates the same metrics for 100 nm GNPs and 120 kVp. As shown in the figure, the values of DALETER range from a minimum of 1.625 to a maximum value of 1.779, while DER values range from 9.8 to 16.85 in the same annular region. The most striking observation of the results is that even though the DER has increased compared with the case of 50 nm GNPs, the values of DALETER have been decreased for all patterns. This can be attributed to the self-absorption of low-energy secondary electrons within GNPs, thereby reducing the average value of LET. However, it is important to note that, similar to the 50 nm case, closely packed patterns provide higher enhancement in LET. In addition, the same patterns discussed earlier (linear two GNPs and triangular) exhibit relatively higher values.

The effect of therapeutic clinical beams is depicted in Fig. 4 where the same metrics are shown for 50 nm GNPs. From the figure, it is readily seen that the values of DER are much less compared to the case of 120 kVp and the same size; likewise, DALETER values decrease, albeit not to the same extent. When compared to each other, the values of DALETER are more pronounced than the corresponding DER for all examined patterns. Nevertheless, the profiles of DER and DALETER are very similar in shape unlike the case of kV beams.

Fig. 5 displays the results for 6 MV beam and 100 nm GNPs. Like the case of 50 nm, the DALETER and DER profiles are of the same shape. Unlike the case of 120 kVp, in which the enhancement in LET decreases with increasing particle size, DALETER values have increased compared with the case of 50 nm GNPs exposed to the same energy. This can be attributed to the increased production of low-energy electrons mainly from the lower energy component of the beam. On the other hand, all the values of DER increased compared to the case of 50 nm GNPs. Table 1 summarizes the results of the simulation presented in this study.

4. Discussion

This study presents a novel approach that aims at a better understanding of GNPs sensitization during radiation therapy. Here, we propose a new metric, LETER, which would bridge the gap between the theoretical predictions of GNPs enhancement and the corresponding observed radiobiological effects, and improve our understanding of the sensitization properties of GNPs. In particular, LETER represents a promising factor that quantifies the enhancement in the linear density of ionizing events along secondary particles tracks. Since the absolute values of LET are fairly low (4.449 and 2.14371 keV/μm for 120 kVp

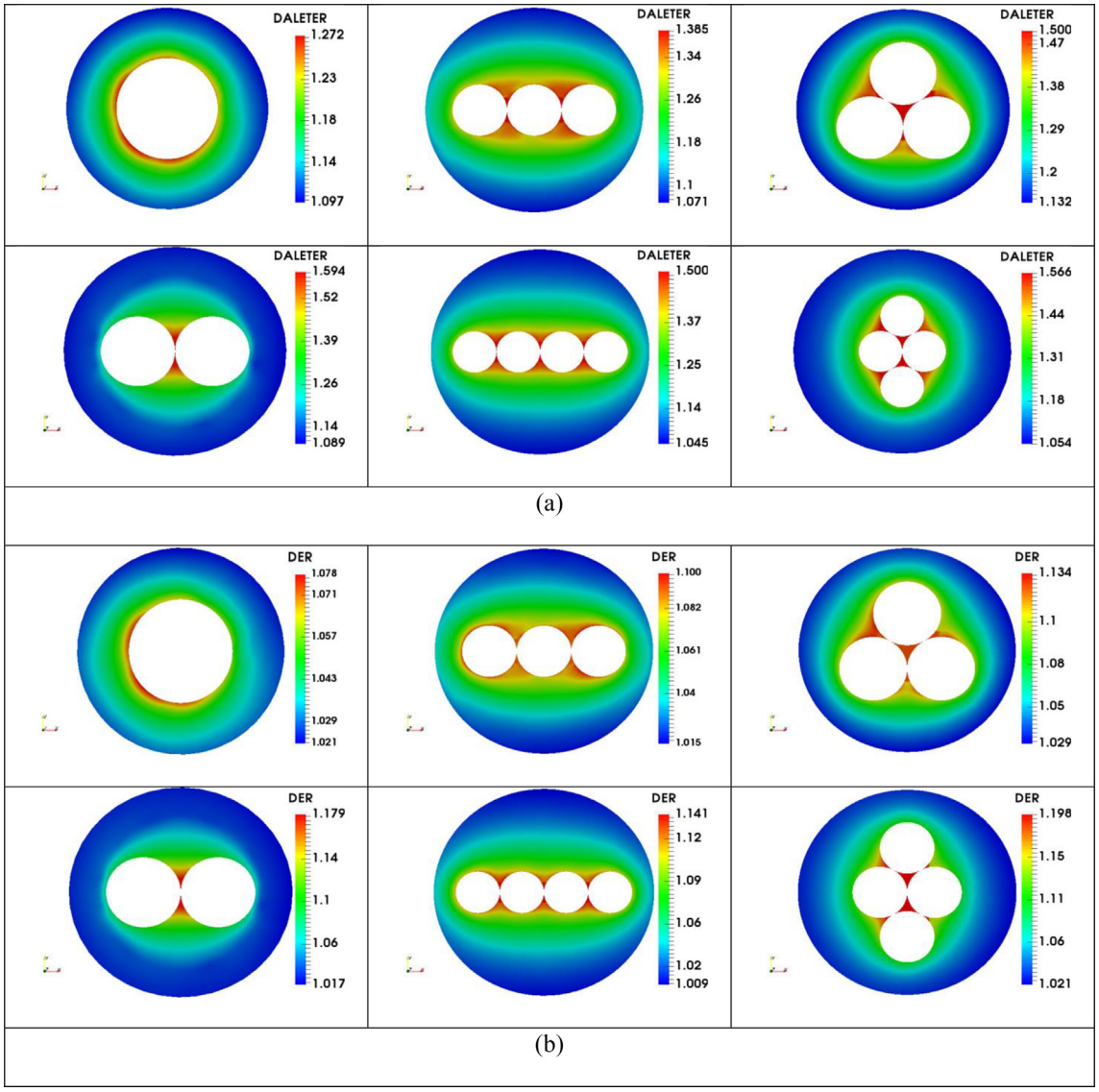

Fig. 4. Different metrics due to electrons in a 25 nm annular region around 50 nm GNP when exposed to 6 MV. (a) DALETER (b) DER.

and 6 MV, respectively), and according to the LET-RBE relationship described in [26], it can be assumed that the LETER is directly correlated with RBE enhancement.

Nonetheless, due to its collective nature, the calculation of LETER is not as straightforward as DER, and in principle, two approaches can be used to calculate the average LET. In the first method, LET is averaged over the relative fluence spectrum of secondary electrons, while in the second one, LET is weighted according to the fraction of dose deposited by secondary electrons. Of greater importance is the latter approach, the originality of this method lies in the fact that DALETER incorporates the calculation of DER implicitly while calculating LETER. Consequently, the dose-averaged LETER is a more suitable metric to predict the radiobiological effects as suggested by Grassbeger et al. [27,28].

During radiation therapy, the presence of GNPs alters the entire phase space of the radiation field in its micrometric vicinity [5,18]. In this perspective, there is a relative increase in the spectrum of secondary electrons, especially in the low energy part due to the emission of low-energy photo- and Auger electrons. Within this energy range, the values of LET of secondary particles are much higher than they are at typical energies of Compton electrons which are dominant in the absence of GNP. This will result in a boost of the average LET (whether using the fluence or the dose approach) in the immediate vicinity of GNPs as proposed by several studies [18,20].

Several radio-sensitization experiments have been conducted for different nanoparticles materials, sizes, concentrations, various incident radiation types and energies [13,29–31]. However, the only study whose parameters fit the energies and GNPs size used in the current work is Chithrani et al. [32]. They found that the sensitization due to 50 nm GNPs when using 105 kVp photons is 1.66 while our predicted value for 120 kVp is in the average range of 1.63–1.81 depending on the clustering pattern and excluding the localized hot-spots. For therapeutic energy range, they reported an enhancement of 1.17 when using 6 MV photons, while our value for 6 MV falls in the average range of 1.18–1.31. This comparison corroborates, in a quantitative way, the claim of the importance of peripheral LETER in adequately predicting the biological impact of GNP radiation.

The purpose of this study is to show the superiority of LETER, compared with DER, in resolving the disconnect between simulations and experimentally observed sensitization in many aspects. First, one of the problems encountered in the enhancement of GNPs is defined by a DER overestimation of the radio-sensitization in the diagnostic energy range, and an underestimation in the therapeutic energy range [12,13]. Remarkably, this disparity can be resolved by studying the LETER

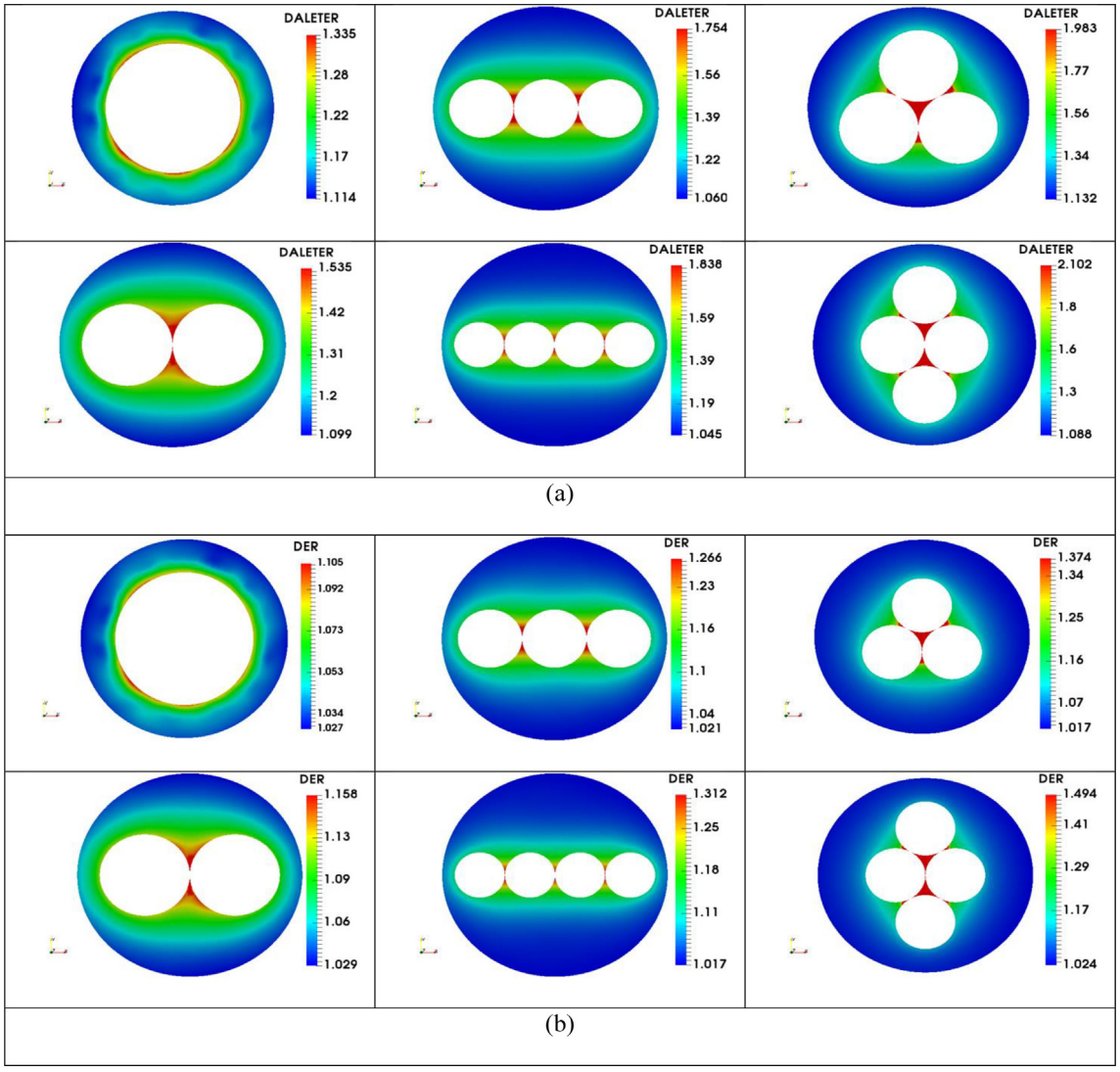

Fig. 5. Different metrics due to electrons in a 25 nm annular region around 100 nm GNP when exposed to 6 MV. (a) DALETER (b) DER.

Table 1
Summary of the simulation results, the first row of each pattern represents the case of 50 nm GNPs, the second row shows the results of 100 nm GNPs.

Clustering pattern	120 kVp		6 MV	
	LETER	DER	LETER	DER
One GNP	1.733–1.806	6.005–11.790	1.097–1.272	1.021–1.078
	1.625–1.726	9.799–16.870	1.114–1.335	1.027–1.105
Tow GNPs	1.696–1.894	6.535–36.220	1.089–1.594	1.017–1.179
	1.467–1.769	8.860–54.540	1.099–1.535	1.029–1.158
Three linear GNPs	1.641–1.873	6.166–37.940	1.071–1.385	1.015–1.100
	1.138–1.742	7.466–55.640	1.060–1.754	1.021–1.266
Three triangular GNPs	1.658–1.947	8.171–48.990	1.132–1.500	1.029–1.134
	1.407–1.779	7.377–70.130	1.132–1.983	1.017–1.374
Four linear GNPs	1.398–1.861	5.273–39.150	1.045–1.500	1.009–1.141
	1.058–1.734	7.305–56.730	1.045–1.838	1.017–1.312
Four rhomboid GNPs	1.633–1.910	7.155–52.830	1.054–1.566	1.021–1.198
	1.293–1.746	8.991–76.610	1.088–2.102	1.024–1.494

instead of DER. According to the results summarized in Table 1, the values of LETER in the kV range are much smaller compared to the calculated DER, while, in the MV range, they are slightly higher than its DER counterparts. Second, it has been reported that the radio-sensitizing effects of GNPs increase with decreasing particle size in the diagnostic energy range [6]. As can be seen from Table 1, the LETER of GNPs having a size of 50 nm is greater than it is for 100 nm (in the case of 120 kVp); in contrast, the values of DER in the case of 100 nm are higher compared with 50 nm GNPs.

Although the main focus of this work was the elucidation of the radio-sensitization properties of GNPs using the new metric LETER, it is worth noting that the study of the magnitude of LET (e.g. in units of keV/μm) is equally important. In a more biologically relevant context, the absolute values of LET can be very beneficial in quantitatively assessing the detailed therapeutic outcome of GNP-mediated radiation therapy. For instance, the values of LET can be used to predict the distribution of reactive oxygen species (ROS) in the vicinity of GNPs.

In the light of the results presented in this study, it is evident that the computed DALETER and DER profiles for a single GNP are anisotropic both radially and angularly, in broad agreement with the findings of Gadoue et al. [5]. In that respect, it has been reported that the DER, electron currents, and all relevant dosimetric quantities in the nanometric vicinity of solitary GNPs are anisotropic, and that the degree of such anisotropy is dependent upon the energy and spectrum of incident photons, and the size of GNP. Moreover, according to the results shown in this study, the agglomerative clustering of GNPs results in a collective response that mitigates the anisotropic nature of dosimetric profiles, as demonstrated by Gadoue et al. [11].

It is worth mentioning that the spectrum of 120 kVp and 6 MV photons used in the current work is limited to specific beam settings that might differ from the spectra used by other groups. This would explain any slight deviation of the calculated DER values in this study from previous results reported in the literature. Particularly, the most important limitation lies in the fact that a 1 keV electron and photon energy cut off has been used in the deterministic computations. Given the G value of the primary radiolytic products of water are expressed in terms of 100 eV, a lower energy cut off is needed in the future for more meticulous LET profiles. Additionally, the present study has only examined two GNP sizes, namely 50 and 100 nm, and two energies; nonetheless, further investigations are desirable to examine a broad range of GNP sizes and materials for different energies.

5. Conclusions

Deterministic computations were used to calculate LET enhancement profiles of secondary electrons in the immediate vicinity of GNPs. It was the main purpose of this paper to draw attention to LETER, a potentially efficacious metric in terms of predicting the biological outcome in GNP aided radiation therapy. More specifically, DALETER is important in the sense that it accounts for the enhancement in the density of the ionizing events triggered by secondary electrons while inherently taking into consideration DER. In this work, it has been demonstrated that DALETER can be used as an attempt to resolve the disparity between observational and computational radio-sensitization of GNPs, in both diagnostic and therapeutic energy range. In general, LET and DALETER profiles provide radio-biologically meaningful information that helps to improve the understanding of the sensitization properties of GNPs.

6. Competing interests

The authors declare that they have no competing interests.

Funding

This research did not receive any specific grant from funding agencies in the public, commercial, or not-for-profit sectors.

Acknowledgments

The authors wish to express their deep gratitude to Dr. Cliff Drum at Sandia National lab for his valuable advice about SCEPTRE. In addition, the authors acknowledge the physics department at the University of Massachusetts Lowell and GHPCC for providing the computational resources needed to run the simulations.

References

[1] Mesbahi A. A review on gold nanoparticles radiosensitization effect in radiation therapy of cancer. Rep Pract Oncol Radiother 2010;15:176–80. https://doi.org/10.1016/j.rpor.2010.09.001.
[2] Cho SH, Jones BL, Krishnan S. The dosimetric feasibility of gold nanoparticle-aided radiation therapy (GNRT) via brachytherapy using low-energy gamma-/x-ray sources. Phys Med Biol 2009;54:4889–905. https://doi.org/10.1088/0031-9155/54/16/004.
[3] Hainfeld JF, Slatkin DN, Smilowitz HM. The use of gold nanoparticles to enhance radiotherapy in mice. Phys Med Biol 2004;49:N309–15. https://doi.org/10.1088/0031-9155/49/18/N03.
[4] Butterworth KT, McMahon SJ, Currell FJ, Prise KM. Physical basis and biological mechanisms of gold nanoparticle radiosensitization. Nanoscale 2012;4:4830–8. https://doi.org/10.1039/c2nr31227a.
[5] Gadoue SM, Toomeh D, Zygmanski P, Sajo E. Angular dose anisotropy around gold nanoparticles exposed to X-rays. Nanomedicine 2017;13:1653–61. https://doi.org/10.1016/j.nano.2017.02.017.
[6] McMahon SJ, Hyland WB, Muir MF, Coulter JA, Jain S, Butterworth KT, et al. Biological consequences of nanoscale energy deposition near irradiated heavy atom nanoparticles. Sci Rep 2011;1:18. https://doi.org/10.1038/srep00018.
[7] Cho SH. Estimation of tumour dose enhancement due to gold nanoparticles during typical radiation treatments: a preliminary Monte Carlo study. Phys Med Biol 2005;50:N163. https://doi.org/10.1088/0031-9155/50/15/N01.
[8] Leung MK, Chow JC, Chithrani BD, Lee MJ, Oms B, Jaffray DA. Irradiation of gold nanoparticles by x-rays: Monte Carlo simulation of dose enhancements and the spatial properties of the secondary electrons production. Med Phys 2011;38:624–31. https://doi.org/10.1118/1.3539623.
[9] Jones BL, Krishnan S, Cho SH. Estimation of microscopic dose enhancement factor around gold nanoparticles by Monte Carlo calculations. Med Phys 2010;37:3809–16. https://doi.org/10.1118/1.3455703.
[10] Li W, Müllner M, Greiter M, Bissardon C, Xie W, Schlatll H, et al. Monte Carlo simulations of dose enhancement around gold nanoparticles used as X-ray imaging contrast agents and radiosensitizers. Medical Imaging 2014: Physics of Medical Imaging: International Society for Optics and Photonics. 2014. p. 90331K.
[11] Gadoue SM, Zygmanski P, Sajo E. The dichotomous nature of dose enhancement by gold nanoparticle aggregates in radiotherapy. Nanomed (Lond) 2018;13:809–23. https://doi.org/10.2217/nnm-2017-0344.
[12] Jain S, Coulter JA, Hounsell AR, Butterworth KT, McMahon SJ, Hyland WB, et al. Cell-specific radiosensitization by gold nanoparticles at megavoltage radiation energies. Int J Radiat Oncol Biol Phys 2011;79:531–9. https://doi.org/10.1016/j.ijrobp.2010.08.044.
[13] Butterworth KT, McMahon SJ, Taggart LE, Prise KM. Radiosensitization by gold nanoparticles: effective at megavoltage energies and potential role of oxidative stress. Transl Cancer Res 2013;2:269–79. https://doi.org/10.3978/j.issn.2218-676X.2013.08.03.
[14] McMahon SJ, Hyland WB, Muir MF, Coulter JA, Jain S, Butterworth KT, et al. CORRIGENDUM: biological consequences of nanoscale energy deposition near irradiated heavy atom nanoparticles. Sci Rep 2013;3:1725. https://doi.org/10.1038/srep00018.
[15] Basu S, Ghosh SK, Kundu S, Panigrahi S, Praharaj S, Pande S, et al. Biomolecule induced nanoparticle aggregation: effect of particle size on interparticle coupling. J Colloid Interface Sci 2007;313:724–34. https://doi.org/10.1016/j.jcis.2007.04.069.
[16] Gustavsson H, Bjack SAJ, Medin J, Grusell E, Olsson LE. Linear energy transfer dependence of a normoxic polymer gel dosimeter investigated using proton beam absorbed dose measurements. Phys Med Biol 2004;49:3847–55. https://doi.org/10.1088/0031-9155/49/17/002.
[17] Guan F, Peeler C, Bronk L, Geng C, Taleei R, Randeniya S, et al. Analysis of the track-and dose-averaged LET and LET spectra in proton therapy using the geant4 Monte Carlo code. Med Phys 2015;42:6234–47. https://doi.org/10.1118/1.4932217.
[18] Garnica-Garza HM. Microdosimetry of X-ray-irradiated gold nanoparticles. Radiat Prot Dosim 2013;155:59–63. https://doi.org/10.1093/rpd/ncs278.
[19] Regulla D, Friedland W, Hieber L, Panzer W, Seidenbusch M, Schmid E. Spatially limited effects of dose and let enhancement near tissue/gold interfaces at diagnostic X ray qualities. Radiat Prot Dosim 2000;90:159–63. https://doi.org/10.1093/oxfordjournals.rpd.a033109.
[20] Zellmer DL, Chapman JD, Stobbe CC, Xu F, Das IJ. Radiation fields backscattered from material interfaces: I. Biological effectiveness. Radiat Res 1998;150:406–15.
[21] Gadoue SM, Toomeh D. Radio-sensitization efficacy of gold nanoparticles in inhalational nanomedicine and the adverse effect of nano-detachment due to coating

inactivation. Phys Med 2019. https://doi.org/10.1016/j.ejmp.2019.02.013.
[22] Bruss DE, Fan WC, Bossler K, Drumm C, Pautz SD, Felice A. Sandia Computational Engine for Particle-Transport Cross Sections v. 0.0. Albuquerque, NM (United States): Sandia National Lab. (SNL-NM); 2017.
[23] Brian C, Franke RPK, Laub Thomas W, Crawford Martin J. The Integrated TIGER Series of Coupled Electron/Photon Monte Carlo Transport Code Revision 4. ITS Version 6. 2009. SAND-2008-3331.
[24] Wilkens JJ, Oelfke U. Analytical linear energy transfer calculations for proton therapy. Med Phys 2003;30:806–15. https://doi.org/10.1118/1.1567852.
[25] Geng C, Gates D, Bronk L, Ma D, Guan F. Physical parameter optimization scheme for radiobiological studies of charged particle therapy. Phys Med 2018;51:13–21. https://doi.org/10.1016/j.ejmp.2018.06.001.
[26] Takatsuji T, Yoshikawa I, Sasaki MS. Generalized concept of the LET-RBE relationship of radiation-induced chromosome aberration and cell death. J Radiat Res 1999;40:59–69. https://doi.org/10.1269/jrr.40.59.
[27] Grassberger C, Paganetti H. Elevated LET components in clinical proton beams. Phys Med Biol 2011;56:6677–91. https://doi.org/10.1088/0031-9155/56/20/011.
[28] Paganetti H, Niemierko A, Ancukiewicz M, Gerweck LE, Goitein M, Loeffler JS, et al. Relative biological effectiveness (RBE) values for proton beam therapy. Int J Radiat Oncol Biol Phys 2002;53:407–21. https://doi.org/10.1016/S0360-3016(02)02754-2.
[29] Mehrnia SS, Hashemi B, Mowla SJ, Arbabi A. Enhancing the effect of 4MeV electron beam using gold nanoparticles in breast cancer cells. Phys Med 2017;35:18–24. https://doi.org/10.1016/j.ejmp.2017.02.014.
[30] Fathy MM, Mohamed FS, Elbialy N, Elshemey WM. Multifunctional chitosan-capped gold nanoparticles for enhanced cancer chemo-radiotherapy: an invitro study. Phys Med 2018;48:76–83. https://doi.org/10.1016/j.ejmp.2018.04.002.
[31] Retif P, Pinel S, Toussaint M, Frochot C, Chouikrat R, Bastogne T, et al. Nanoparticles for radiation therapy enhancement: the key parameters. Theranostics 2015;5:1030–44. https://doi.org/10.7150/thno.11642.
[32] Chithrani DB, Jelveh S, Jalali F, van Prooijen M, Allen C, Bristow RG, et al. Gold nanoparticles as radiation sensitizers in cancer therapy. Radiat Res 2010;173:719–28. https://doi.org/10.1667/RR1984.1.